JJMIE

Volume 4, Number 2, March. 2010
ISSN 1995-6665
Pages 286 - 291

Jordan Journal of Mechanical and Industrial Engineering

Computational Modelling for Solid-State Variable-Frequency Induction Motor Drive - II

Saleh A. Al-Jufout [a,*], Kamal A. Khandakji [b]

[a] Tafila Technical University, Faculty of Engineering, Department of Electrical Engineering,
[b] Yanbu Industrial College, Department of Electrical and Electronics Technology

Abstract

This contribution describes a computational model of the solid-state variable-frequency induction motor drive. The model of the induction motor has been represented as a system of differential equations for flux linkages and angular velocity. These equations have been represented in Cartesian coordinate system, the use of which decreased their number to 7 instead of 10 equations and restricted the use of the model only for symmetrical conditions of operation. The output voltages applied to the terminals of the motor have been given according to voltage-versus-frequency patterns of constant V/f^2 and constant $V/f^{(1/2)}$. This model has been developed for both transient and steady-state conditions analyses. The waveforms of the current and electromagnetic torque of the motor during sudden acceleration and deceleration have been illustrated and analyzed.

Keywords: Induction Motor; Mathematical Modelling; Solid-State; Variable-Frequency.

1. Introduction

Industrial electronic control, in its wide sense, includes all methods used to control the performance of an engineering system; and has gained a wide acceptance in power technology. When applied to machinery, it involves the starting, acceleration, reversal, deceleration and stopping of a motor and the attached load.

Loads attached to the induction motor may vary greatly. Some of them, like fans, require very little torque at starting or running at low speeds; and have torques which increase as the square of speed.

Other loads might be harder to start, requiring more than rated full-load torque of the motor to get the load moving, such as in hoisting mechanism. Until the advent of modern solid-state drives, induction motors (IM) in general were not the suitable machines for applications requiring considerable speed control.

The method of choice, today, for induction motor speed control, is the solid-state variable-frequency induction motor drive (VFD).

Recently, many papers are devoted to the variable-frequency drives. In Ref. [1], field tests at five sites showed that the pump performance at the reduced speed using VFD could reasonably match the throttled conditions at a reduced horsepower demand. Ref. [2] introduces the application principles, describes the optimal methods of stack sizing, and presents an example which showed that multi-stack and VFD techniques can reduce both the make-up airflow rate and fan energy in the constant speed fan exhaust system. In Ref. [3], a comparison was conducted between on/off and VFD systems to control greenhouse ventilation fans where the results show that the VFD system has a greater potential to reduce the range of amplitude variations in the air temperature and humidity ratio within the greenhouse.

The solid-state variable-frequency induction motor drive provides a variety of voltage-versus-frequency patterns that can be selected to match the torque from the induction motor to the torque required by its load.

At 14th European Simulation Multiconference (ESM'2000) held in May, 2000 in Belgium, the first author of this paper presented a paper entitled: "Computational Modelling for Solid-State Variable-Frequency Induction Motor Drive" [4], in which the output voltages applied to the terminals of the motor had been given according to the general-purpose standard voltage-versus-frequency pattern (*V/f=constant)*. Where the output voltage linearly changes with changes in the output frequency for speeds below the base speed and holds the output voltage constant for speeds above the base speed.

To complete the work done in Ref. [4], in this paper, the output voltages applied to the terminals of the induction motor are given according to the voltage-versus-frequency patterns of $V/f^2=constant$ and $V/f^{(1/2)}=constant$. Thus this paper is entitled the same as Ref. [4], but with index (II): "Computational Modelling for Solid-State Variable-Frequency Induction Motor Drive - II".

* Corresponding author. drjufout@ttu.edu.jo.

2. Mathematical Modelling

The three-phase, deep-bar cage induction motor can be mathematically modeled by representing it as a system of differential equations for flux linkages and angular velocity. To take in account the skin effect, the rotor is represented as two parallel-connected resistive-inductive circuits.

To decrease the number of differential equations, the model of the motor is represented in Cartesian coordinate system instead of the phase coordinates, thus the system of differential equations comprises 7 equations instead of 10. This approach decreases the time of computations, but restricts the use of the model only for symmetrical modes of operation [5]. The differential equations can be expressed in orthogonal axes (α, β) as follows [6]:

$$\frac{d\lambda_{S\alpha}}{dt} = v_{S\alpha} - \frac{R_S}{L_{\sigma S}}(\lambda_{S\alpha} - \lambda_{\mu\alpha}) \quad (1)$$

$$\frac{d\lambda_{S\beta}}{dt} = v_{S\beta} - \frac{R_S}{L_{\sigma S}}(\lambda_{S\beta} - \lambda_{\mu\beta}) \quad (2)$$

$$\frac{d\lambda_{R\alpha}^{(1)}}{dt} = -\frac{R_R^{(1)}}{L_{\sigma R}^{(1)}}(\lambda_{R\alpha}^{(1)} - \lambda_{\mu\alpha}) - \omega\,\lambda_{R\beta}^{(1)} \quad (3)$$

$$\frac{d\lambda_{R\beta}^{(1)}}{dt} = -\frac{R_R^{(1)}}{L_{\sigma R}^{(1)}}(\lambda_{R\beta}^{(1)} - \lambda_{\mu\beta}) + \omega\,\lambda_{R\alpha}^{(1)} \quad (4)$$

$$\frac{d\lambda_{R\alpha}^{(2)}}{dt} = -\frac{R_R^{(2)}}{L_{\sigma R}^{(2)}}(\lambda_{R\alpha}^{(2)} - \lambda_{\mu\alpha}) - \omega\,\lambda_{R\beta}^{(2)} \quad (5)$$

$$\frac{d\lambda_{R\beta}^{(2)}}{dt} = -\frac{R_R^{(2)}}{L_{\sigma R}^{(1)}}(\lambda_{R\beta}^{(2)} - \lambda_{\mu\beta}) + \omega\,\lambda_{R\alpha}^{(2)} \quad (6)$$

$$\frac{d\omega}{dt} = \frac{1}{J}(\tau_e - \tau_m) \quad (7)$$

where

$\lambda_{S\alpha}, \lambda_{R\alpha}^{(1)}, \lambda_{R\alpha}^{(2)}, \lambda_{S\beta}, \lambda_{R\beta}^{(1)}, \lambda_{R\beta}^{(2)}$ - The flux linkages of the stator and the rotor circuits in α, β coordinates respectively;

$R_S, R_R^{(1)}, R_R^{(2)}$ - The resistances of the stator and the rotor circuits respectively;

$L_{\sigma S}, L_{\sigma R}^{(1)}, L_{\sigma R}^{(2)}$ - The leakage inductances of the stator and the rotor circuits respectively;

$v_{S\alpha}, v_{S\beta}$ - The applied voltages in α, β coordinates respectively;

$\lambda_{\mu\alpha}, \lambda_{\mu\beta}$ - The flux linkages of the magnetization branch in α, β coordinates respectively;

ω - The angular velocity of the motor;

J - The combined rotor and mechanical load inertia;

τ_e, τ_m - The electromagnetic and the mechanical torque respectively.

The electromagnetic torque and the flux linkages of the magnetization branch can be calculated as follows:

$$\tau_e = \frac{1}{L_{\sigma S}}\left[\lambda_{S\beta}\sum_{i=1}^{2} k_R^{(i)}\lambda_{R\alpha}^{(i)} - \lambda_{S\alpha}\sum_{i=1}^{2} k_R^{(i)}\lambda_{R\beta}^{(i)}\right] \quad (8)$$

$$\lambda_{\mu\alpha} = k_S\lambda_{S\alpha} + \sum_{i=1}^{2} k_R^{(i)}\lambda_{R\alpha}^{(i)} \quad (9)$$

$$\lambda_{\mu\beta} = k_S\lambda_{S\beta} + \sum_{i=1}^{2} k_R^{(i)}\lambda_{R\beta}^{(i)} \quad (10)$$

Where the contribution coefficients can be calculated as follows:

$$k_S = \frac{1}{L_{\sigma S}}\left[\frac{1}{L_{\sigma S}} + \frac{1}{L_\mu} + \sum_{i=1}^{2}\frac{1}{L_{\sigma R}^{(i)}}\right]^{-1} \quad (11)$$

$$k_R^{(1)} = \frac{1}{L_{\sigma R}^{(1)}}\left[\frac{1}{L_{\sigma S}} + \frac{1}{L_\mu} + \sum_{i=1}^{2}\frac{1}{L_{\sigma R}^{(i)}}\right]^{-1} \quad (12)$$

$$k_R^{(2)} = \frac{1}{L_{\sigma R}^{(2)}}\left[\frac{1}{L_{\sigma S}} + \frac{1}{L_\mu} + \sum_{i=1}^{2}\frac{1}{L_{\sigma R}^{(i)}}\right]^{-1} \quad (13)$$

where

L_μ - The inductance of the magnetization branch.

The stator currents can be calculated as follows:

$$i_{S\alpha} = \frac{\lambda_{S\alpha} - \lambda_{\mu\alpha}}{L_{\sigma S}} \quad (14)$$

$$i_{S\beta} = \frac{\lambda_{S\beta} - \lambda_{\mu\beta}}{L_{\sigma S}} \quad (15)$$

The above mentioned differential equations can be solved by fourth-order Runge-Kutta method [7]. The equivalent circuit parameters (resistances and inductances) can be defined in per unit (p.u.) by engineering methods [8, 9]. And the mechanical load can be either a constant or as a function of the angular velocity. To simulate the solid-state variable-frequency drive, it is suggested that the applied voltages to be given according to the voltage-versus-frequency pattern of V/f^2=*constant* as follows:

$$v_a = k_d V_{\max}\sin(\sqrt{k_d}\,\omega t) \quad (15)$$

$$v_b = k_d V_{\max}\sin(\sqrt{k_d}\,\omega t - 120^o) \quad (16)$$

$$v_c = k_d V_{\max}\sin(\sqrt{k_d}\,\omega t - 240^o) \quad (17)$$

where

k_d - the scaling coefficient:

$0 < k_d \leq 1$

The phase voltages can be represented in Cartesian coordinate system as follows:

$$v_\alpha = v_a \quad (18)$$

$$v_\beta = \frac{v_b - v_c}{\sqrt{3}} \quad (19)$$

The mechanical torque is given as a function of the angular velocity:

$$\tau_m = f(\omega) \quad (20)$$

To simulate the drive according to the voltage-versus-frequency pattern of $V/f^{(1/2)}=constant$, it is suggested that (15), (16) and (17) to be replaced by the following equations:

$$v_a = k_d V_{\max} \sin(k_d{}^2 \omega t) \quad (21)$$

$$v_b = k_d V_{\max} \sin(k_d{}^2 \omega t - 120^o) \quad (22)$$

$$v_c = k_d V_{\max} \sin(k_d{}^2 \omega t - 240^o) \quad (23)$$

3. Case Study

In this section, starting with low frequency followed by sudden acceleration and starting with rated frequency followed by sudden deceleration are simulated.

This case study is modeled and simulated for both voltage-versus-frequency patterns ($V/f^2=constant$ and $V/f^{(1/2)}=constant$).

Fig. 1, and Fig. 2, show, respectively, the phase currents and electromagnetic torque of the motor during starting with 50-Hz frequency followed by a sudden deceleration to the half of the rated speed according to the pattern of $V/f^2=constant$. As shown from Fig. 1, the inrush current during direct on-line starting is about 8.42 p.u. and the starting duration is about 0.76 s. Then suddenly the applied voltages are changed to 25% of the rated with a frequency of 25 Hz that simulates a sudden deceleration from the rated speed to half of the rated. The inrush current associated with this sudden deceleration is about 6.53 p.u. Fig. 2 shows the electromagnetic torque of the motor from which it is obvious that the inrush starting torque is about 2.41 p.u. and is about 4.12 p.u. at the sudden deceleration. Here the negative torque indicates that the motor operates in the second quadrant (generation mode) until it loses the extra kinetic energy stored in its rotor. The motor should be protected from these large values of currents and electromagnetic torque, thus this process is performed through independently adjustable acceleration and deceleration ramps mainly controlled by time. Fig. 3 and Fig. 4 show the same values shown in Fig. 1 and Fig. 2, but during starting by applying 25% of the rated voltage with 25-Hz frequency followed by a sudden acceleration to the rated speed. By comparing the starting processes, it is obvious that, in the later case, it is softer and longer.

The sudden acceleration is also associated with large inrush values of current (7.46 p.u.) and electromagnetic torque (2.88 p.u.), while the motor operates in the first quadrant during all the process time.

It is noticed also from these figures that the developed model can be used for both transient and steady-state conditions. The steady-state values of the phase currents and electromagnetic torque are different after both sudden acceleration and deceleration because the mechanical torque is given as a function of the angular velocity.

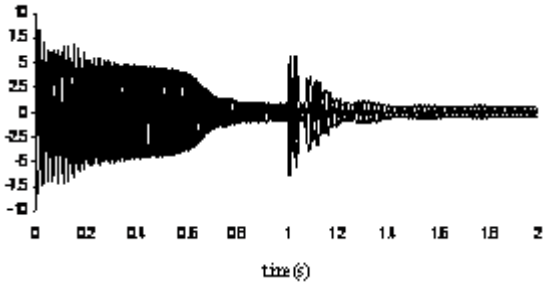

Figure 1. Phase currents of IM in p.u. during starting with 50-Hz frequency followed by a sudden deceleration to the half of the rated speed where the voltage is applied according to the pattern of $V/f^2=constant$.

Fig. 5 and Fig. 6 show, respectively, the phase currents and electromagnetic torque of the motor during starting by applying 50-Hz rated voltages followed by a sudden deceleration to the half of the rated speed according to the pattern of $V/f^{(1/2)}=constant$.

As shown from Fig. 5, the inrush current at the sudden deceleration is about 10.68 p.u., while the inrush electromagnetic torque is about 8.79 p.u. (Fig. 6).

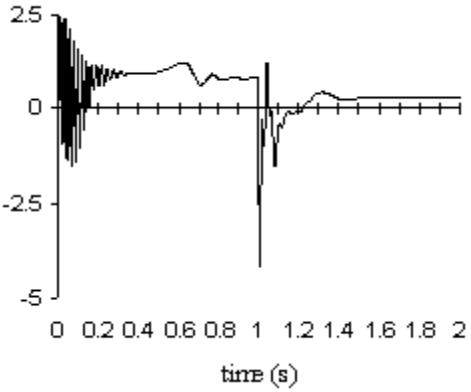

Figure 2. Electromagnetic torque of IM in p.u. during starting with 50-Hz frequency followed by a sudden deceleration to the half of the rated speed where the voltage is applied according to the pattern of $V/f^2=constant$

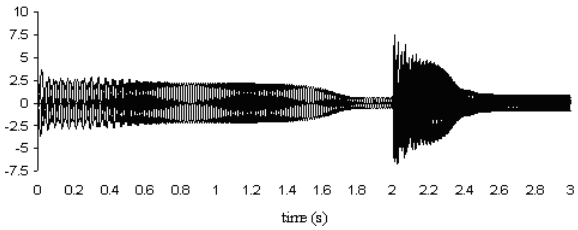

Figure 3. Phase currents of IM in p.u. during starting with 25-Hz frequency followed by a sudden acceleration to the rated speed where the voltage is applied according to the pattern of V/f^2=*constant*.

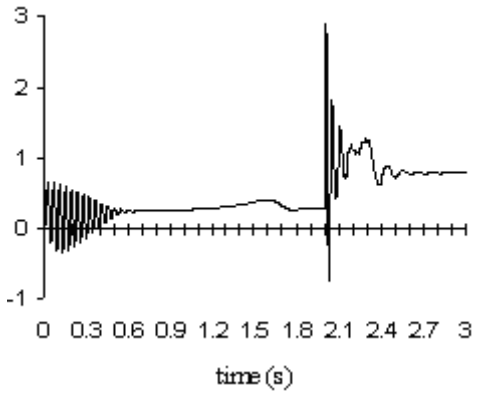

Figure 4. Electromagnetic torque of IM in p.u. during starting with 25-Hz frequency followed by a sudden acceleration to the rated speed where the voltage is applied according to the pattern of V/f^2=*constant.*

Fig. 7 and Fig. 8 show the same values shown in Fig. 5 and Fig. 6, but the applied voltages, during starting, are 70.7% of the rated with 25-Hz frequency. When Comparing Fig. 3 with Fig. 7, it is obvious that the starting duration, in the later, is shorter because the applied voltages are 70.7% of the rated.

It is noticed also that this starting duration is shorter than in the case of full-voltage starting of Fig. 1 and Fig 5,because of the dependence of the mechanical load on the angular velocity.

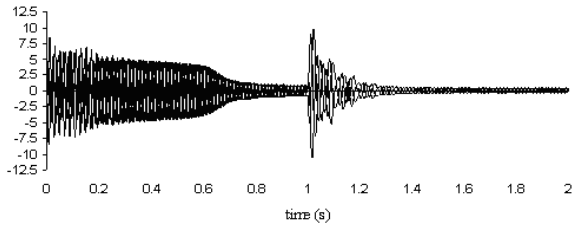

Figure 5. Phase currents of IM in p.u. during starting with 50-Hz frequency followed by a sudden deceleration to the half of the rated speed where the voltage is applied according to the pattern of $V/f^{(1/2)}$=*constant.*

Practically, when the desired speed of the motor is changed, the solid-state variable-frequency controlling it will also change the voltage and frequency to bring the motor to the new operating speed. If the change is sudden, the drive does not try to make the motor instantaneously jump to the new desired speed. Instead, the rate of the induction motor acceleration or deceleration is limited to safe rates by special circuits built into the electronics of the solid-state drive. These rates can be adjusted independently for accelerations and decelerations.

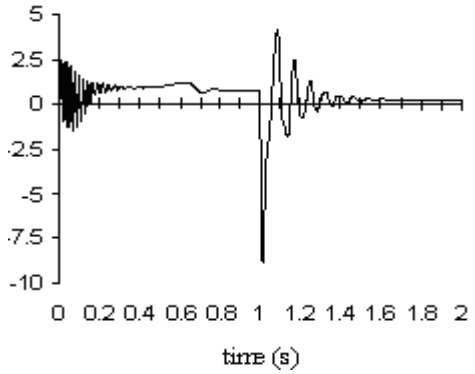

Figure 6. Electromagnetic torque of IM in p.u. during starting with 50-Hz frequency followed by a sudden deceleration to the half of the rated speed where the voltage is applied according to the pattern of $V/f^{(1/2)}$= *constant.*

The results of the assumed case study and their analysis can be used for condition analysis, determining the independent rates of accelerations and decelerations for a certain drive with a certain mechanism and load characteristic, and for engineering education.

Here also the importance of computational modelling and simulation can be obviously noticed since the assumed case study cannot be performed experimentally due to the dangerous consequences of sudden acceleration and deceleration.

Finally, the obtained results confirm that the processes of sudden acceleration and deceleration are associated with undesirable large values of inrush currents and electromagnetic torques.

Avoiding these large values is performed by limiting the rate of acceleration or deceleration to a safe level that can be adjusted independently by the use of the developed model.

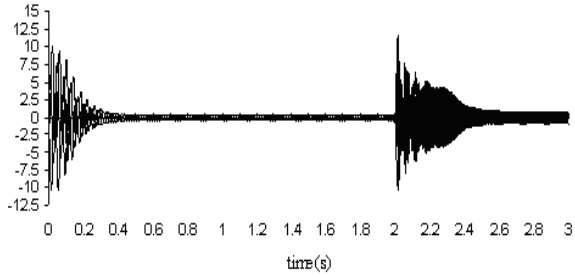

Figure 7. Phase currents of IM in p.u. during starting with 25-Hz frequency followed by a sudden acceleration to the rated speed where the voltage is applied according to the pattern of $V/f^{(1/2)}$=*constant*

4. Conclusion

The computational model of the solid-state variable-frequency induction motor drive is developed. The model of the induction motor is represented as a system of differential equations for flux linkages and angular velocity. These equations are represented in Cartesian coordinate system, the use of which decreases their number to 7 instead of 10 equations and restricts the use of the model only for symmetrical conditions of operation.

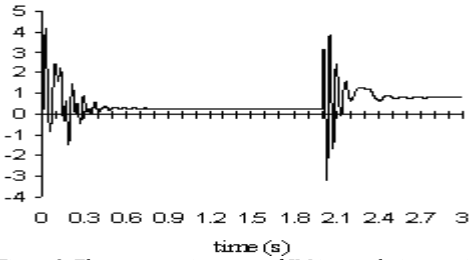

Figure 8. Electromagnetic torque of IM in p.u. during starting with 25-Hz frequency followed by a sudden acceleration to the rated speed where the voltage is applied according to the pattern of $V/f^{(1/2)}=constant$.

The starting process followed by sudden acceleration or deceleration according to two different voltage-versus-frequency patterns ($V/f^{2}=constant$ and $V/f^{(1/2)}=constant$) are simulated and the corresponding waveforms of the phase currents and electromagnetic torque are illustrated and analyzed. The obtained results confirm that the processes of sudden acceleration and deceleration are associated with undesirable large values of inrush currents and electromagnetic torques. Avoiding these large values is performed by limiting the rate of acceleration or deceleration to a safe level by special circuits built into the electronics of the solid-state drive. The developed model is recommended for optimum determination of these rates.

References

[1] B. Hanson, C. Weigand, S. Orloff, "Performance of electric irrigation pumping plants using variable frequency drives". Journal of Irrigation and Drainage Engineering. Vol. 122, No. 3, 1996, 179-182.

[2] G. Wang, M. Liu, Y. Cui, D. Yuill, "Retrofit constant speed fan laboratory exhaust systems using multi-stack and variable frequency drive techniques". Journal of Solar Energy Engineering. Vol. 126, No. 1, 2004, 610-613.

[3] M. Teitel, Y. Zhao, M. Barak, E. Bar-lev, D. Shmuel, "Effect on energy use and greenhouse microclimate through fan motor control by variable frequency drives". Energy Conversion and Management. Vol. 45, No. 1, 2004, 209-223.

[4] S. Al-Jufout, "Computational modelling for solid-state variable-frequency induction motor drive". 14th European Simulation Multiconference, Ghent, Belgium, 2000.

[5] S. Al-Jufout, "Fault simulation by hypothetical stub moving along medium-length transmission line". 13th IEEE Mediterranean Electrotechnical Conference, Benalmadena, Spain, 2006.

[6] S. Al-Jufout, "Modelling of the cage induction motor for symmetrical and asymmetrical modes of operation". Computers and Electrical Engineering. Vol. 29, No. 11, 2003, 851-860.

[7]Richard L, Douglas J. Numerical analysis. 7th ed. Brooks/Cole Publishing Company, Kentucky: Florence; 2002.

[8] Sivokobylenko V. Transients in multi-machine power supply systems of power stations. DonNTU, Ukraine: Donetsk; 1984.

[9]Sivokobylenko V, Kostenko V. Electrical motors mathematical modelling of the power station auxiliaries. DonNTU, Ukraine: Donetsk; 1979.